nature geoscience
LETTERS
PUBLISHED ONLINE: XX MONTH XXXX | DOI: 10.1038/NGEO730

Significant effect of sediment cohesion on delta morphology

Douglas A. Edmonds[1]* and Rudy L. Slingerland[2]

The morphologies of the world's deltas are thought to be determined by river discharge, tidal range and wave action[1]. More recently, sea level rise[2,3] and human engineering[4] have been shown to shape delta evolution. The effects of factors such as sediment type and the overall amount of sediment carried by rivers are considered secondary[4–6]. In particular, the role of sediment cohesion, which is controlled by sediment size and type of vegetation, is unclear. Here we use a numerical flow and transport model[7–10] to show that sediment cohesiveness also strongly influences the morphology of deltas. We find that, holding all other factors constant, highly cohesive sediments form bird's-foot deltas with rugose shorelines and highly complex floodplains, whereas less cohesive sediments result in fan-like deltas with smooth shorelines and flat floodplains. In our simulations, sediment cohesiveness also controls the number of channels that form within the deltas, and the average angle of bifurcation of those channels. As vegetation generally acts as a cohesive agent, we suggest that deltas that formed before the expansion of land plants in the Devonian period should show fan-like characteristics, a finding consistent with the limited data from the sedimentological record[11].

The roles of sediment properties and vegetation as controls of delta morphodynamics have been explored by only a few field studies[5,6,12,13], physical tank experiments[14,15] and numerical models[16]. Together these studies suggest that cohesiveness can affect delta morphology, but it is unclear why and to what extent. Here we conduct morphodynamic simulations using Delft3D (v. 3.28) by varying the cohesiveness of the sediment and the relative flux of cohesive to non-cohesive sediment while holding all other factors constant (see the Methods section for modelling details). Thirty simulations of delta growth were conducted in which a steady river discharge of 1,000 $\mathrm{m^3\,s^{-1}}$ carries equilibrium concentrations of cohesive and non-cohesive sediment into a standing body of water devoid of waves, tides and buoyancy. Cohesive transport is calculated though the advection–diffusion equation with erosion and deposition treated as source and sink terms, the magnitudes of which are determined by a critical shear stress for erosion ($\tau_{\mathrm{ce(C)}}$) and deposition ($\tau_{\mathrm{cd(C)}}$). The cohesiveness of sediment is defined as a normalized excess shear stress $\tau_{\mathrm{N}} = (\overline{\tau_{\mathrm{o}}} - \tau_{\mathrm{ce(C)}})/(\overline{\tau_{\mathrm{o}}})$, where $\overline{\tau_{\mathrm{o}}}$ ($\mathrm{N\,m^{-2}}$) is the temporally and spatially averaged basal shear stress at the river inlet and $\tau_{\mathrm{ce(C)}}$ ($\mathrm{N\,m^{-2}}$) is the critical shear for erosion of the cohesive sediment fraction. For the same fluid shear stress a smaller τ_{N} reflects sediment that is more cohesive. To capture the dependence of $\tau_{\mathrm{ce(C)}}$ on sediment type, deposit age, permeability, vegetation type, organic matter and pore-water composition[17], we varied $\tau_{\mathrm{ce(C)}}$ over a range consistent with its natural variation (Table 1). The proportion of cohesive silt and clay relative to non-cohesive sand is defined as $Q_{\mathrm{sr}} = (\overline{Q_{\mathrm{s(C)}}})/(\overline{Q_{\mathrm{s(N)}}})$, where $\overline{Q_{\mathrm{s(C)}}}$ and $\overline{Q_{\mathrm{s(N)}}}$ are the time-averaged sediment fluxes ($\mathrm{m^3\,s^{-1}}$) at the river inlet of the cohesive and non-cohesive sediment fractions, respectively. Q_{sr} is varied by changing the median grain size of the non-cohesive fraction or the incoming concentration of cohesive sediment (Table 1). In our experiments, the same morphological effect occurs if τ_{N} is varied for a fixed Q_{sr} or vice versa. Therefore, for simplicity we refer to changes in cohesion as movement along the upper-left to lower-right diagonal of Fig. 1a. For example, bulk cohesion increases from the lower right to the upper left (Fig. 1a).

In each experiment a self-formed delta and distributary network are generated by the same processes observed in field studies: (1) growth of a subaqueous platform; (2) development of subaqueous levees and river mouth bars[17]; (3) mouth bar stagnation and subsequent channel bifurcation[18,19]; (4) subaqueous dissection of mouth bars and levees into multiple bifurcations[20]; and (5) subaerial channel avulsion[21] (see Supplementary Movies M1 and M2 for examples of these processes). We argue that the modelled deltas are representative of real deltas because the discharge ratios between bifurcate channels typically range from 1 to 6, comparable to measured variation in the field[22], the differences in bed heights of the bifurcate arms scale with the discharge ratio between the two bifurcates[23] and flood maps of our modelled deltas are spatially similar to observed flood maps on deltas from the Dartmouth Flood Observatory[4]. Furthermore, if discharge is varied while holding sediment type constant, the numbers of channels and delta size roughly follow regression relationships derived from 51 natural deltas[6].

Experimental results are compared after the same volume of sediment has been transported into the basin and before the channels prograde to the edges of the computational domain. Figure 1b shows that deltas with low τ_{N} are elongate/bird's foot-like because their deposition is confined to a limited area, which produces an irregular deposit with a rugose shoreline. The channels are long and weakly sinuous, and the floodplains are complex with preserved channel scars and bays (Fig. 1b, upper left). Deltas with greater τ_{N} are fan-like because they fill the available space resulting in a roughly axisymmetric deposit with smoother shorelines. The channels are straight and the floodplains are topographically smooth with few bays and preserved channel scars (Fig. 1b, lower right). The cumulative number of channel bifurcations created in a delta and the average bifurcation angle also depend strongly on the strength and relative volume of cohesive sediment (Fig. 2a,b).

In our experiments, the presence of cohesion induces morphological change through two effects. An increase in cohesive sediment reduces the ability of the system to re-erode deposited sediment, making river mouth bars and levees more stable. Furthermore, compared with low-cohesion channels at the same discharge, high-cohesion channels tend to be deeper, which changes the structure of the turbulent jet at the river mouth. The relative importance of these

[1]Saint Anthony Falls Laboratory, Department of Geology and Geophysics, University of Minnesota, Minneapolis, Minnesota 55416, USA, [2]Department of Geosciences, The Pennsylvania State University, 513A Deike Bldg, University Park, Pennsylvania 16802, USA. *e-mail: dedmonds@umn.edu.

NATURE GEOSCIENCE DOI: 10.1038/NGEO730

Table 1 | Model parameters and results for modelling experiments used in this study.

Run ID	$D50_N$ (μm)	[COH] (kg m^{-3})	$\tau_{ce(C)}$ (N m^{-2})	τ_o (N m^{-2})	$Q_{s(C)}$ (m^3 s^{-1})	$Q_{s(N)}$ (m^3 s^{-1})	Cumulative number of bifurcations/avulsions	Average α in time and space (°)
a	125	0.20	0.50	5.18	0.0792	0.0168	23/0	82
b	125	0.20	2.00	7.30	0.0718	0.0086	18/4	76
c	225	0.20	1.00	5.46	0.0744	0.0067	27/5	65
d	350	0.20	0.50	5.96	0.0754	0.0071	20/2	79
e	350	0.20	2.00	7.57	0.0717	0.0062	18/2	70
f	225	0.42	0.50	6.21	0.1544	0.0100	17/1	78
g	225	0.42	0.80	7.32	0.1608	0.0111	22/5	75
h	225	0.42	0.25	5.83	0.1582	0.0147	15/0	77
i	225	0.20	0.50	4.79	0.0754	0.0102	27/2	74
j	225	0.50	2.00	9.47	0.1799	0.0085	6/1	66
k	125	0.20	0.80	5.28	0.0745	0.0105	26/5	77
l	350	0.35	0.80	6.38	0.1286	0.0062	16/2	67
m	225	0.42	0.10	5.77	0.1707	0.0214	8/0	82
n	350	0.20	0.80	5.21	0.0747	0.0057	27/4	64
o	125	0.08	0.10	4.22	0.0347	0.0288	6/0	96
p	125	0.08	1.00	4.80	0.0299	0.0171	26/3	75
q	290	0.35	1.70	8.27	0.1274	0.0061	14/3	65
r	225	0.42	1.20	7.95	0.1521	0.0087	20/4	72
s	225	0.70	1.50	9.76	0.2458	0.0104	10/4	60
t	125	0.13	1.00	5.31	0.0487	0.0129	24/4	72
u	125	0.13	2.00	6.82	0.0481	0.0114	18/5	70
v	225	0.33	2.00	8.64	0.1176	0.0080	17/3	65
w	225	0.50	2.60	10.46	0.1780	0.0094	3/0	69
x	350	0.35	2.60	10.68	0.1119	0.0066	11/5	72
y	125	0.20	0.25	4.66	0.0776	0.0193	16/0	81
z	350	0.50	0.80	7.30	0.1809	0.0073	12/2	68
aa	225	0.55	0.50	6.85	0.1997	0.0104	12/4	79
bb	350	0.18	0.80	5.10	0.0655	0.0061	24/5	75
cc	225	0.10	2.00	6.33	0.0370	0.0087	13/4	68
dd	125	0.20	1.55	6.70	0.0741	0.0081	16/4	73

*Median grain size of non-cohesive fraction.
† Concentration of cohesive sediment at the inlet.
‡ Critical erosive shear stress of the cohesive sediment fraction.
§ Time-averaged bed shear stress of the incoming flow.
|| Time-averaged sediment discharge of the cohesive and non-cohesive fraction at the inlet, respectively.
¶ Measurement error on average bifurcation angle is ±2°.

effects changes as the amount of cohesion varies in the experiments, which leads to different delta morphologies.

At low cohesion fewer bifurcations form because there is enough excess shear stress for the turbulent jet at the river mouth to re-erode the bar basinward instead of the bar stagnating and causing a bifurcation[19] (Fig. 1b, lower left; Fig. 2a). Even when mouth bars stagnate, the resulting bifurcations are usually unstable because as the bar expands laterally, the subaqueous levees flanking the bar are easily eroded, and the flows down the bifurcate arms must turn increasingly larger angles (Fig. 2b) leading to closure of one arm[24]. Low-cohesion deltas are fan-like because the levees are weak and easily eroded, and sediment and water are fed to nearly the whole delta topset through numerous crevasses. Avulsions are infrequent (Table 1) because the shoreline roughly progrades basinward uniformly and no single obvious cross-levee slope advantages arise.

At intermediate cohesion the greatest number of bifurcations forms because all of the channel-creating processes described above participate in network construction (Fig. 1b, middle; Fig. 2a). The deposits are harder to erode because they have a higher percentage of cohesive sediment, which has a higher $\tau_{ce(C)}$. This causes more frequent river mouth bar stagnation and channel splitting. The levees are stronger and less easily eroded, which counterbalances the laterally expanding bar and stabilizes bifurcations near the optimal angle for efficient flow[25] (Fig. 2b). As the levees are more resistant to erosion they aggrade to the surface, confine the flow and cause sediment deposition basinward of the levee termini, resulting in progradation of channels into the basin and a rugose shoreline. In some cases bifurcations are abandoned during this process and the channel progrades around the relic mouth bars resulting in sinuous planform geometries with many enclosed bays on the floodplain (Fig. 3). The resulting high cross-levee slopes create more avulsions (Table 1), consistent with the observation that cohesive experimental deltas are dominated by avulsion[14,26].

At high cohesion, bird-foot deltas with few channels form because avulsions and dissections of mouth bars are strongly inhibited (Fig. 1b, upper right; Fig. 2a). Resistant levees create a narrow channel and a highly concentrated erosive jet that is able to recycle the mouth bar basinward causing channel progradation far into the basin (Fig. 1). As the effect of progradation is strong, the planform pattern is dominantly sinuous as channels readily prograde around relic bifurcations (Fig. 3). Competent levees decrease avulsion frequency (Table 1) even though cross-levee slopes become high.

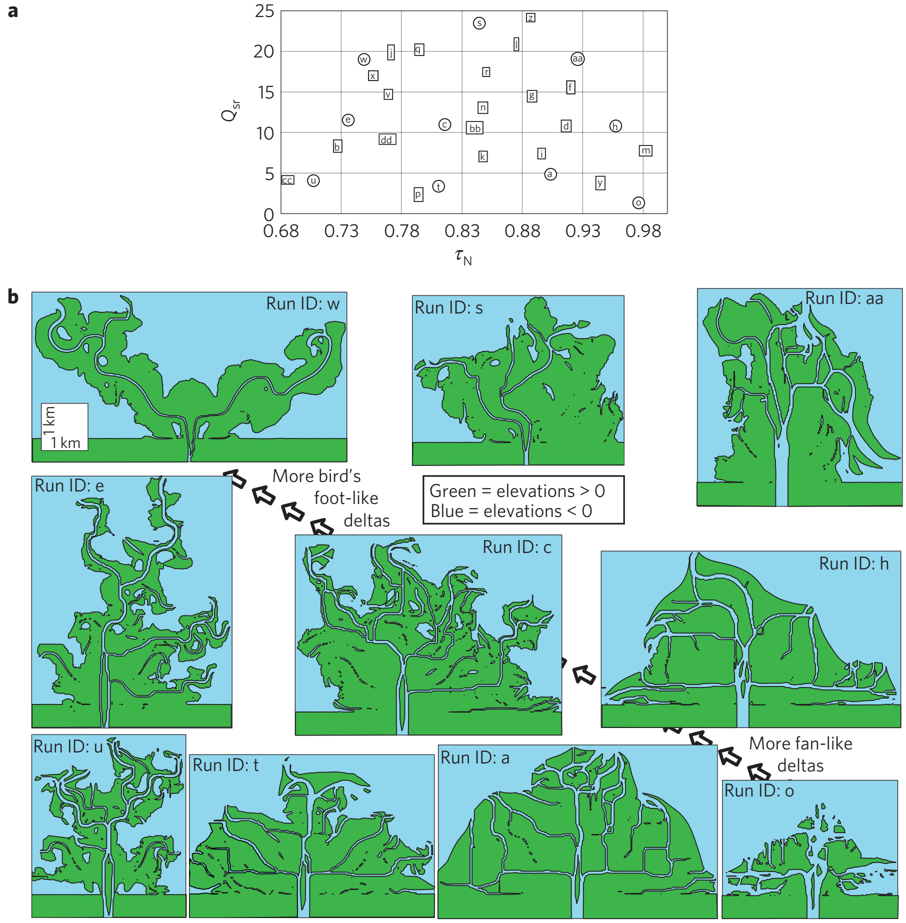

Figure 1 | Shoreline traces of deltas created in this study. a, Parameter space explored in this study. The letters refer to the different experiments in Table 1 and the circled letters correspond to the tracings pictured. The bulk cohesion of the delta deposit increases from lower right to upper left. **b**, The relative positions of the tracings reflect their position in parameter space where total cohesion increases from bottom right to upper left.

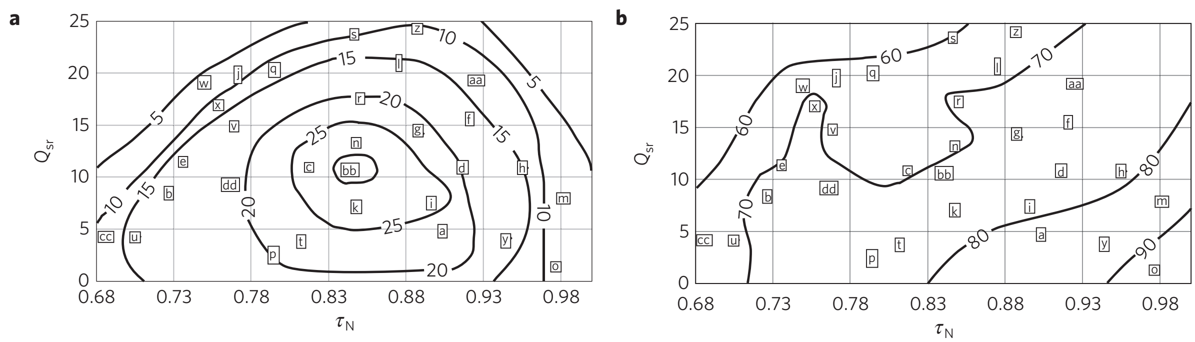

Figure 2 | Cumulative number of bifurcations and average bifurcation angle as a function of cohesiveness. a,**b**, Hand-contoured maps of the cumulative number of bifurcations created (letter indicates run ID) and space- and time-averaged bifurcation angle (in degrees). A bifurcation is defined as flow divergence created by two or more bifurcate channels that have subaerial levees and transport water and sediment. The greatest cumulative number of bifurcations (and therefore channels) occurs at intermediate cohesion. The bifurcation angle is the angle formed by the upstream intersection of bifurcate channels' centrelines. An increase in cohesion causes a decrease in bifurcation angle. Table 1 contains the cumulative number of bifurcations and the average angle for each run.

These results can be used to understand the morphological differences among river-dominated deltas. Recently, Syvitski and Saito[6] showed that the number of distributary channels covering a delta depends on maximum monthly discharge and inversely on marine power. They also showed that rivers with higher discharges (for example, the Amazon, Mekong, Mississippi and Orinoco rivers) deliver finer-grained sediment to their deltas. We suggest that part of the correlation between the number of distributaries and discharge is due to cohesive properties of the sediment that construct the deltas. For example, the Mississippi and Yellow river deltas should have similar channel network morphologies because they possess similar discharges and marine powers[6]. Yet, these deltas are not similar; the Mississippi delta has a rugose shoreline and 71 channels, whereas the Yellow river delta has a smooth shoreline and only five channels[6]. There is a fourfold difference in pre-dam Q_{sr} between the two deltas (11.5 for the Mississippi and

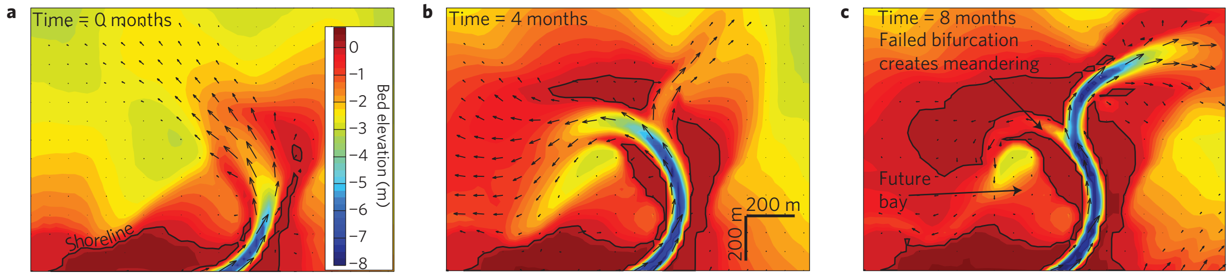

Figure 3 | Serial images from Run b showing how sinuosity and inter-bend bays form. a, Initial channel curvature creates an asymmetric mouth bar with a steeper bed slope and more offshore accommodation space to the left. **b**, More water and sediment are transported there and the accommodation space is filled as deposition approaches the shoreline. **c**, A bend is created when the left channel is abandoned in favour of the right channel, which now has a steeper gradient. A bay will form as additional sedimentation closes the gap between shorelines in the left channel. Velocity vectors are shown for every third cell and for scale the velocity magnitude in the channel is ∼1 m s^{-1}.

2.8 for the Yellow river; see Supplementary Information for how these numbers were calculated), suggesting that the morphological difference could be due to sediment properties alone. The idea that sediment cohesion controls the bird's-foot morphology of the Mississippi delta is consistent with the findings of Kim *et al.*[27], who suggest an abundance of mud and strong levees are an important condition for the formation of an elongate delta.

Sediment cohesion exerts an important control on delta network formation by stabilizing levees, river mouth bars and bifurcations. In fact, its effect on such delta attributes as the number of distributary channels and shoreline rugosity is as important as river, wave and tidal energies. Bird's-foot to fan-delta shapes, which have traditionally been explained by invoking different river and wave climates[1], can be created by changing only the proportion of cohesive sediment delivered to the delta head and the critical shear stress for erosion of the cohesive fraction.

Furthermore, these results can be broadly interpreted to suggest that the presence and type of vegetation could also have an important role in delta morphology because vegetation generally acts as a cohesive agent. If true, Earth's deltas older than the rise of land plants in the Devonian should show more fan-like characteristics with fewer channels, bays and delta plain lakes. This is consistent with observations from the Precambrian[11] and Taconian shoreline deposits of eastern North America.

These results also have immediate implications for current delta restoration efforts. On the Mississippi delta, where land loss is considerable, it has been suggested that opening levee diversions[28] could halt land loss. However, for that strategy to be viable these results indicate that the proportions of cohesive and non-cohesive sediment must be controlled to maximize the amount of subaerial delta created per unit volume of sediment (compare the lower right and upper left of Fig. 1b), lobe shape, length of shoreline and number of channels, all of which determine the suitability of that habitat for flora and fauna.

Methods

Delft3D simulates fluid flow and morphological changes at timescales from seconds to years and has been validated for a wide range of hydrodynamic, sediment transport and scour and deposition applications in rivers, estuaries and tidal basins, including the self-formed evolution of rivers and tidal deltas[7–10]. Our runs were computed using the depth-averaged, nonlinear, shallow-water equations derived from the three-dimensional Reynolds-averaged Navier–Stokes equations for incompressible free surface flow. The horizontal eddy-viscosity coefficient is defined as the combination of the subgrid-scale horizontal eddy-viscosity, computed from a horizontal large-eddy simulation, and the background horizontal viscosity here set equal to 0.001 m^2 s^{-1}.

A basin of 300 by 225 computational cells, each 25 m^2, is positioned at the Equator with an initial bed slope of 0.000375 to the north, creating initial depths from 1 to 3.5 m similar to the bathymetry of Atchafalaya Bay, Louisiana . Initial depths are then adjusted from 0 to 5 cm using a white-noise model to simulate natural variations. Bed roughness is set to a spatially and temporally constant Chezy value of 45 m$^{1/2}$ s^{-1}. A rectangular river channel 250 m wide and 2.5 m deep extending 1,000 m basinward is carved into a 500-m-wide subaerial, sandy shoreline along the southern boundary of the grid (see initial conditions in the Supplementary Movies). Tests showed that the shoreline width and the distance the channel initially extends into the basin do not alter the results. Western, northern and eastern boundaries are open with a temporally constant water surface elevation equal to zero. Five metres of evenly mixed sediment (50% cohesive and 50% non-cohesive) are initially available for erosion of the bed.

In Delft3D cohesive sediment is defined as silt-sized and finer (<64 μm) and can be transported only in suspension. In all experiments reported here the cohesive sediment size is medium-grained silt (30 μm). Cohesive transport is calculated though the advection–diffusion equation with erosion and deposition treated as source and sink terms, the magnitudes of which are based on the Partheniades–Krone formulation. The user must specify a critical shear stress for erosion ($\tau_{ce(C)}$) and deposition ($\tau_{cd(C)}$) of the cohesive fraction. The existence of $\tau_{ce(C)}$ is widely accepted, whereas the existence of $\tau_{cd(C)}$ is still debated[29]. Current evidence suggests that while $\tau_o > \tau_{ce(C)}$ cohesive sediment deposition either occurs constantly, because $\tau_{cd(C)} \gg \tau_{ce(C)}$ (ref. 30), or is mutually exclusive from erosion because $\tau_{ce(C)} \gg \tau_{cd(C)}$ (ref. 29). In a reach where $\tau_o > \tau_{ce(C)}$, specifying mutually exclusive erosion and deposition means cohesive sediment erosion will occur until $\tau_o < \tau_{ce(C)}$, making the resultant equilibrium form highly dependent on the choice of $\tau_{ce(C)}$ and the initial cohesive sediment thickness. To circumvent this problem, our runs specify constant sediment deposition by setting $\tau_{cd(C)} = 1{,}000$ N m^{-2}, so that equilibrium depth occurs when the erosive flux equals the depositional flux.

Non-cohesive sediment is defined as sand-sized and coarser (>64 μm) and can be transported as suspended or bed load. The size of the non-cohesive fraction was varied throughout the runs (Table 1). The transport formulation is from Van Rijn (see Delft3D handbook for full reference) and erosion and deposition shear stresses are based on the Shields curve. All cohesive and non-cohesive grains are assumed to have a density of 2,650 kg m^{-3}. Suspended sediment eddy diffusivities are a function of the fluid eddy diffusivities and are calculated using horizontal large-eddy simulation and grain settling velocity. The effect of bedslope on bed load transport vectors is taken into account.

A bed stratigraphy model containing 25 layers tracks the evolution of the bed sediment, thereby allowing for spatial variation in erosion caused by the presence of mud or sand at the surface. A time step of 9 s was adopted to obey all stability criteria. We sped up bed adjustments by multiplying the bed sediment flux in each time step by a morphological scale factor of 175. To avoid numerical instabilities caused by supercritical flow in shallow areas a grid cell is considered dry if its depth is shallower than 10 cm. Delft3D uses a boundary fitted grid so all erosion and deposition fluxes are applied to the bottom cell face. Thus, channel widening can occur only when dry grid cells adjacent to the channel are wetted and eroded.

Each model run is computed through >10^5 time steps, making it possible that small errors could become magnified leading to spurious results. To assess the sensitivity of delta morphology, we conducted replicate experiments for a few runs in Table 1 and varied the time step, the magnitude of white noise on the bed and the sweep direction of the numerical scheme. We found that varying each of these leads to a different solution in the details but the gross-scale morphology and number of channels created in the delta are not affected.

Received 30 September 2009; accepted 24 November 2009; published online XX Month XXXX

References

1. Galloway, W. E. in *Deltas: Models for Exploration* (ed. Broussard, M. L.) 87–98 (Houston Geological Society, 1975).
2. Jerolmack, D. J. Conceptual framework for assessing the response of delta channel networks to Holocene sea level rise. *Quart. Sci. Rev.* (2009).

3. Giosan, L. *et al*. Young Danube delta documents stable Black Sea level since the middle Holocene: Morphodynamic, paleogeographic, and archaeological implications. *Geology* **34,** 757–760 (2006).
4. Syvitski, J. P. M. *et al*. Sinking deltas due to human activities. *Nature Geosci.* **2,** 681–686 (2009).
5. Orton, G. J. & Reading, H. G. Variability of deltaic processes in terms of sediment supply, with particular emphasis on grain size. *Sedimentology* **40,** 475–512 (1993).
6. Syvitski, J. & Saito, Y. Morphodynamics of deltas under the influence of humans. *Glob. Planet. Change* **57,** 261–282 (2007).
7. Lesser, G., Roelvink, J., Van Kester, J. & Stelling, G. Development and validation of a three-dimensional morphological model. *Coast. Eng.* **51,** 883–915 (2004).
8. Dastgheib, A., Roelvink, J. A. & Wang, Z. B. Long-term process-based morphological modeling of the Marsdiep tidal basin. *Mar. Geol.* **256,** 90–100 (2008).
9. van Maren, D. S. Grain size and sediment concentration effects on channel patterns of silt-laden rivers. *Sedim. Geol.* **202,** 297–316 (2007).
10. Marciano, R., Wang, Z. B., Hibma, A., de Vriend, H. J. & Defina, A. Modeling of channel patterns in short tidal basins. *J. Geophys. Res.* **110,** doi:10.1029/2003JF000092 (2005).
11. Eriksson, P. G. *et al*. Precambrian clastic sedimentation systems. *Sedim. Geol.* **120,** 5–53 (1998).
12. Coleman, J. M. *Deltas: Processes and Models of Deposition for Exploration* (Bergess, CEPCO Division, 1981).
13. Jerolmack, D. J. & Mohrig, D. Conditions for branching in depositional rivers. *Geology* **35,** 463–466 (2007).
14. Hoyal, D. & Sheets, B. A. Morphodynamic evolution of experimental cohesive deltas. *J. Geophys. Res.* **114** (2009).
15. Martin, J., Sheets, B., Paola, C. & Hoyal, D. Influence of steady base-level rise on channel mobility, shoreline migration, and scaling properties of a cohesive experimental delta. *J. Geophys. Res.* **114** (2009).
16. Seybold, H. *et al*. Simulation of birdfoot delta formation with application to the Mississippi Delta. *J. Geophys. Res.* **114** (2009).
17. Black, K. S., Tolhurst, T. J., Paterson, D. M. & Hagerthey, S. E. Working with natural cohesive sediments. *J. Hydraul. Eng.* **128,** 2 (2002).
18. Wright, L. D. Sediment transport and deposition at river mouths: A synthesis. *Geol. Soc. Am. Bull.* **88,** 857–868 (1977).
19. Edmonds, D. A. & Slingerland, R. L. Mechanics of river mouth bar formation: Implications for the morphodynamics of delta distributary networks. *J. Geophys. Res.* **112** (2007).
20. Wellner, R., Beaubouef, R. T., Van Wagoner, J. C., Roberst, H. H. & Sun, T. Jet-plume depositional bodies—the primary building blocks of Wax Lake delta. *Gulf Coast Associat. Geol. Soc. Trans.* **55,** 867–909 (2005).
21. Coleman, J. M. Dynamic changes and processes in the Mississippi River delta. *Geol. Soc. Am. Bull.* **100,** 999–1015 (1988).
22. Edmonds, D. A. & Slingerland, R. L. Stability of delta distributary networks and their bifurcations. *Wat. Resour. Res.* **44** (2008).
23. Zolezzi, G., Bertoldi, W. & Tubino, M. in *Braided Rivers: Process, Deposits, Ecology and Management* (eds Bristow, C., Petts, G., Best, J. & Smith, G. S.) 233–256 (Blackwell, 2006).
24. Mosselman, E., Huisink, M., Koomen, E. & Seijmonsbergen, A. C. *River Geomorphology* 235–249 (Wiley, 1995).
25. Keshavarzi, A. & Habibi, L. Optimizing water intake angle by flow separation analysis. *Irrigation Drainage* **54,** 543–552 (2005).
26. Edmonds, D. A., Hoyal, D., Sheets, B. A. & Slingerland, R. L. Predicting delta avulsions: Implications for coastal wetland restoration. *Geology* **37,** 759–762 (2009).
27. Kim, W., Dai, A., Muto, T. & Parker, G. Delta progradation driven by an advancing sediment source: Coupled theory and experiment describing the evolution of elongated deltas. *Wat. Resour. Res.* **45** (2009).
28. Kim, W., Mohrig, D., Twilley, R., Paola, C. & Parker, G. Is it feasible to build new land in the Mississippi River Delta? *Eos Trans. AGU* **90** (2009).
29. Maa, J. P. Y., Kwon, J. I., Hwang, K. N. & Ha, H. K. Critical bed-shear stress for cohesive sediment deposition under steady flows. *J. Hydraul. Eng.-ASCE* **134,** 1767–1771 (2008).
30. Sanford, L. P. & Halka, J. P. Assessing the paradigm of mutually exclusive erosion and deposition of mud, with examples from upper Chesapeake Bay. *Mar. Geol.* **114,** 37–57 (1993).

Acknowledgements

The authors would like to acknowledge financial support from NSF grant EAR-0809653, and the Donors of the American Chemical Society Petroleum Research Fund for support of this research. D.A.E. was supported by the STC Program of the National Science Foundation through the National Center for Earth-Surface Dynamics under agreement EAR-0120914. We thank D. Hoyal, B. Sheets and G. Parker for discussions about deltas and cohesion. The focus of this manuscript greatly benefited from reviews by J. Syvitski and D. Jerolmack.

Author contributions

D.A.E. designed and conducted the numerical modelling and analyses. D.A.E. and R.L.S. critically analysed the results and wrote the paper.

Additional information

The authors declare no competing financial interests. Supplementary information accompanies this paper on www.nature.com/naturegeoscience. Reprints and permissions information is available online at http://npg.nature.com/reprintsandpermissions. Correspondence and requests for materials should be addressed to D.A.E.

Page 1

Query 1: Line no. 1

Please note that the e-mail address of the second author has been removed because as per journal style, only the e-mail address of the corresponding author is allowed.

Page 2

Query 2: Line no. 1

The footnotes of table 1 are not assigned to any of the entries in the table. Please check.

Query 3: Line no. 21

Comma added before 'which' here. OK?

Page 3

Query 4: Line no. 1

Apostrophe added to give 'bifurcate channels' centrelines' in the third last sentence of figure 2's caption. OK?

Query 5: Line no. 3

The style guide states: 'In general, avoid using authors' names and phrases such as 'A. N. Author has shown that' in the text. For example, say 'Water flows downhill2' rather than, 'Garwin has shown2 that water flows downhill.' There are occasions when this rule can be broken, for example when two authors' results are being compared or when the significance of an author's contribution needs emphasis.' Please check the use of 'Syvitski and Saito' (then 'They') here, and 'Kim et al' below.

Page 4

Query 6: Line no. 1

According to style, 'additional' should be changed to 'extra', 'further' or 'more'. Which is most appropriate in the second last sentence of figure 3's caption?

Query 7: Line no. 107

Please provide volume and page range for ref. 2.

Page 5

Query 8: Line no. 21

Please provide page range for refs 10, 14–17, 19, 22 and 27.